Nonlinear Model for Sub- and Superharmonic Motions of a MDOF Moored Structure, Part 2—Sensitivity Analysis and Comparison

S. C. S. Yim
Professor
Coastal and Ocean Engineering Program,
Department of Civil Engineering, Oregon State University,
Corvallis, OR 97331

S. Raman
Project Engineer
Skillings-Connolly, Inc.,
5016 Lacey Boulevard S.E.,
Lacey, WA 98503

P. A. Palo
Naval Facilities Engineering Service Center,
1100 23rd Avenue,
Port Hueneme, CA 93043

The nonlinear R-MI/SO system identification procedure and the parameters of the MDOF system identified in Part 1 are examined in detail in this paper. A parametric study is conducted and the results are presented on the sensitivity of the system parameters for two key nonlinear responses—subharmonic and superharmonic resonances. The parameters are compared to determine the appropriateness of using a single set of system parameters for both response regions. A detailed comparison of the MDOF and the corresponding SDOF system results is performed. The knowledge gained from the SDOF and MDOF studies on the applicability of the R-MISO technique for the system identification of MDOF submerged moored structures is discussed. The results show that the MDOF extension of the R-MI/SO nonlinear system identification technique works well; the resulting system parameters are relatively constant and can be applied to the both the sub- and superharmonic regions. [DOI: 10.1115/1.2073187]

Introduction

In Part 1 [1] of this two-part study, the nonlinear system identification methodology developed earlier by the authors for a single-degree-of-freedom (SDOF) system using the reverse-multi-input/single-output (R-MISO) technique was extended to a multi-degree-of-freedom (MDOF), submerged, moored structure with surge and heave motions. The physical MDOF system model and the formulation of the R-MISO system identification technique were presented. The corresponding numerical algorithm was then developed and applied to the experimental data of the MDOF system to identify the system parameters. In this study, the resulting model is employed for a detailed analysis of the MDOF experimental system and is compared with the results and observations of the SDOF system.

Using the measured wave excitation and response data together with the identified system parameters, a detailed study is performed on the response behavior of the MDOF system. A sensitivity analysis is conducted to determine the optimal range of system parameters and understand the effect of varying the stiffness and damping coefficients on the system response. Then the response behavior of MDOF system is compared to that of the SDOF system based on the individual response behavior and the R-MI/SO technique application.

For the MDOF experimental system considered, the dominant fundamental frequency is $f=0.226$ Hz (corresponding to a fundamental period of $T=4.42$ s) (see Part 1). In this Part 2 study, both subharmonic motions, corresponding wave excitation frequency of $f=0.452$ Hz (period $T=2.21$ s) and superharmonic motions, corresponding to excitation frequency $f=0.113$ Hz (period $T=8.84$ s) will be examined.

For convenience and clarity of reference, all figures and tables in Part 1 and Part 2 are distinguished by that same initial number. All equations referenced in this paper appeared in Part 1.

Contributed by the Ocean Offshore and Arctic Engineering Division of ASME for publication in the JOURNAL OF OFFSHORE MECHANICS AND ARCTIC ENGINEERING. Manuscript received September 26, 2004; final manuscript received March 24, 2005. Assoc. Editor: Ge (George) Wang.

MDOF System Subharmonic Response Behavior

In Part 1, the multipoint moored experimental structure considered was formulated as a general MDOF surge–heave, hydrodynamically damped and excited nonlinear oscillator. A nonlinear-structure nonlinearly damped (NSND) model was then developed and system parameters were identified using the measured wave and subharmonic system motion response data. In order to obtain an optimal range of system parameters, a sensitivity analysis is conducted and the effects of variations in the Keulegan–Carpenter (KC_F) and the Reynolds (Re_F) number are examined in this section.

Sensitivity Analysis. Each system parameter identified in Part 1 using the R-MI/SO technique and subharmonic motion response experimental data was varied over a range in specific increments while keeping all the other identified parameters constant [Table 1(*b*)]. The surge and heave responses are simulated for each parameter coefficient set variation by solving Eqs. (1), (3), and (4). The results are compared in both time and frequency domains. The suitable range and the most suitable value of system parameters are tabulated in Table 1. The table shows that the best value for the system parameters remain the same for all the data, but MH (multi-degree-of-freedom, high wave excitation amplitude) has a restricted range compared to MM1 and MM2 (multi-degree-of-freedom, medium wave excitation amplitude).

The next step is to numerically simulate the system responses using these identified coefficients and the measured wave elevation time histories. It is noted that numerical instability for MH using the 0.0625 s time step to solve the ordinary differential equations, Eqs. (1), (3), and (4) was encountered. By reducing the time step by one-fourth and interpolating the wave force at the intermediate points, a solution was obtained. The observations from the sensitivity analysis are summarized through spectral diagrams in the following paragraphs. Since the datasets MM1 and MM2 exhibit similar behavior, the mean of the resulting spectra for each variation is obtained and used for the comparison.

The effects of varying the coefficient of the linear term, a_1, in the surge force component on heave and surge responses for MM

Table 1 Identified system parameters from the sensitivity analysis of the MDOF subharmonic data

Data	MM1	MM2	MH
a_1 (N/m)	157.8–193.2 (173.9)	154.6–196.4 (177.1)	157.8–189.9 (173.9)
a_2 (N/m^2)	264.0–405.7 (334.9)	259.2–417.6 (340.8)	328.4–334.9 (328.4)
a_3 (N/m^3)	157.8–1725.9 (940.2)	155.5–1710.4 (932.9)	1806.4–1961.0 (1883.7)
b_1 (N/m)	157.8–189.0 (173.9)	157.8–207.5 (175.3)	167.4–183.5 (173.9)
b_3 (N/m^3)	157.8–1255.8 (705.2)	157.8–1255.8 (706.4)	689.1–785.7 (721.3)
c_{12} (N/m^3)	157.8–3606.4 (1883.7)	157.8–3629.4 (1883.7)	1883.7–2009.3 (1944.9)
c_{21} (N/m^3)	157.8–3606.4 (1883.7)	157.8–3629.4 (1883.7)	1883.7–1993.2 (1944.9)
$C_{d1,3}$	0.30–0.65 (0.43)	0.30–0.65 (0.43)	0.43–0.47 (0.45)
$\zeta_{1,3}$ (%)	1.0–4.0 (3.0)	1.0–4.0 (3.0)	2.8–3.2 (3.0)
$f_{n1,3}$ (Hz)	0.28	0.28	0.29

and MH are presented in Fig. 1. The spectral density normalized with the variance of the corresponding wave data (S_{xxn}) is plotted against frequency for a_1 from 58.0 to 217.4 N/m or a1n (the ratio of the instantaneous value of a_1 to the best value of a_1 as given in Table 1) from 0.33 to 1.25. The heave response does not change significantly for MM, whereas in the secondary resonance region, the MH response increases with the increase in a_1. From the surge response behavior, it can be observed from Figs. 1(*b*) and 1(*d*) that there is a slight increase in the primary resonance energy as a_1 increases. The subharmonic resonance region increases and shifts toward the right as a_1 increases for surge and heave.

When the coefficient of the quadratic term, a_2, in the surge force is increased from 0 to 476.6 N/m^2, or a2n from 0 to 1.25, the response in the secondary resonance region for surge increases and decreases for heave slightly for MM, as given in Figs. 2(*a*) and 2(*b*). The effects are more pronounced for MH [Figs. 2(*b*) and 2(*d*)]. The primary resonance region is not significantly affected with the increase in a_2; these three observations are consistent with expectations since the quadratic component force is shifted to twice the fundamental frequency. Figure 3 shows that increasing the coefficient of the cubic term, a_3, in the surge force component from 0 to 1568.1 N/m^3 or a3n from 0 to 2.5, decreases the subharmonic response and the variation is more prominent for MH.

The effects of varying the coefficient of the linear term, b_1, in the heave force component from 116.0 to 231.8 N/m on the heave and surge responses for MM and MH are similar to those of varying the coefficient of the linear term, a_1, in the surge force component. The surge response (not shown here for page limitation; see [2] for details) is observed to be unaffected for MM, whereas the response in the secondary resonance region decreases with increasing b_1 for MH. For the heave response, it is observed that the response in the primary resonance region increases and

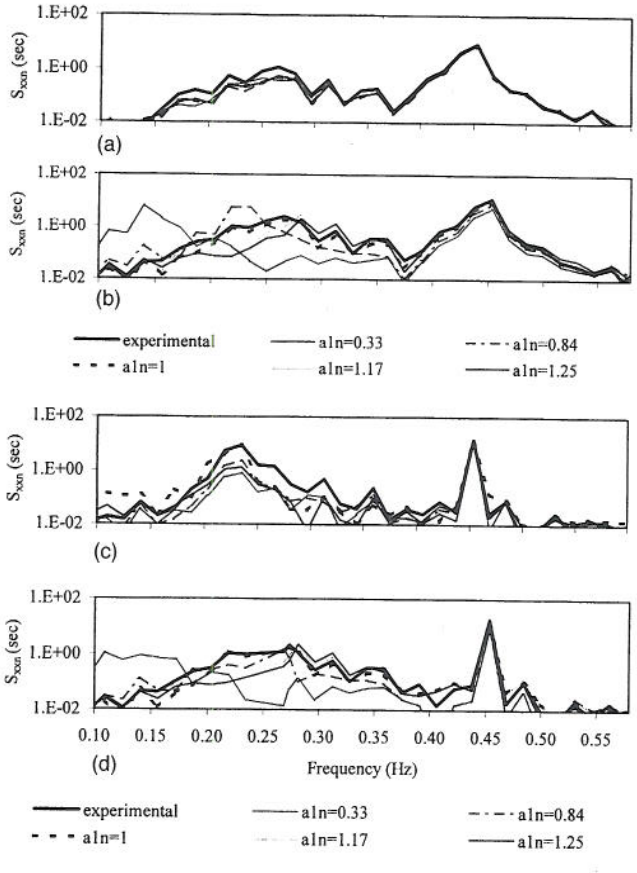

Fig. 1 Effect of a_1 on MDOF system behavior: (*a*) (first) MMH, (*b*) (second) MMS, (*c*) (third) MHH, (*d*) (fourth) MHS

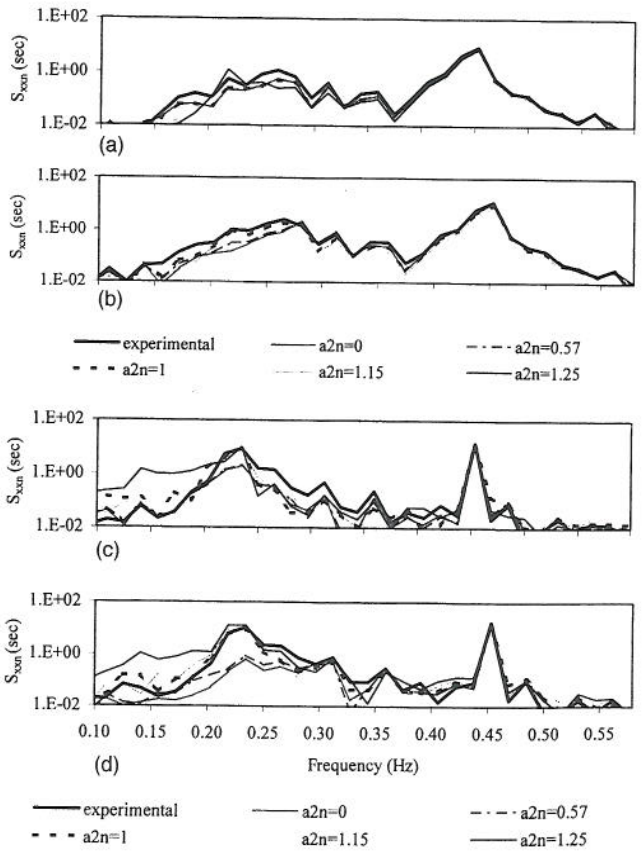

Fig. 2 Effect of a_2 on MDOF system behavior: (*a*) (first) MMH, (*b*) (second) MMS, (*c*) (third) MHH, (*d*) (fourth) MHS

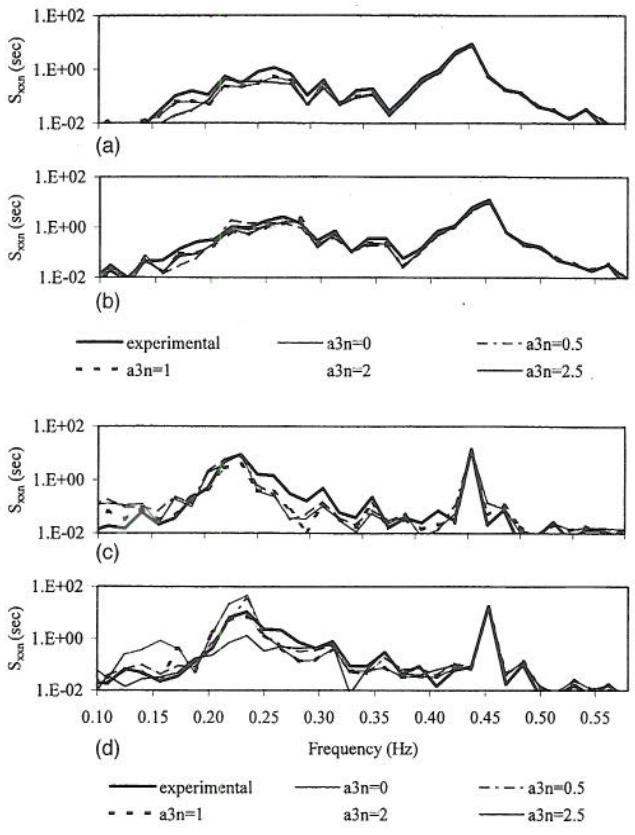

Fig. 3 Effect of a_3 on MDOF system behavior: (*a*) (first) MMH, (*b*) (second) MMS, (*c*) (third) MHH, (*d*) (fourth) MHS

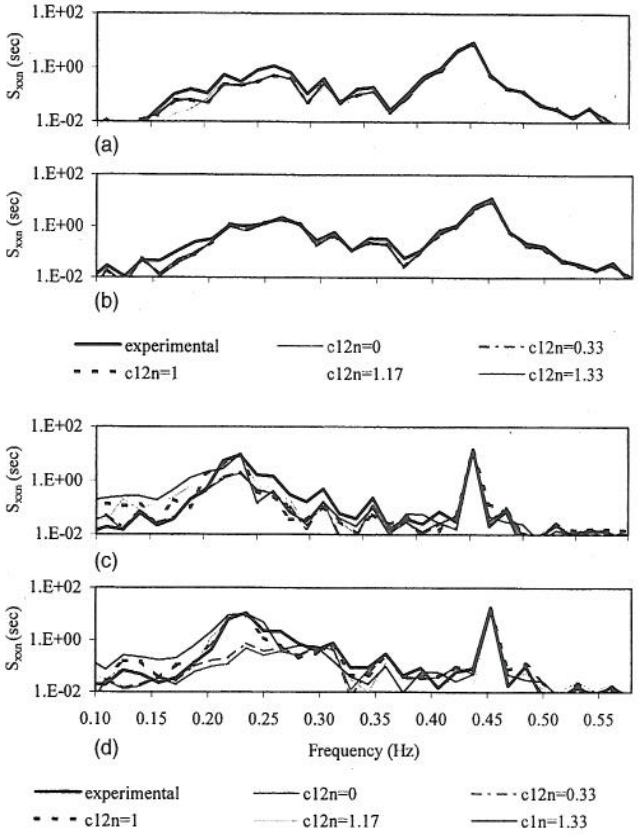

Fig. 4 Effect of c_{12} on MDOF system behavior: (*a*) (first) MMH, (*b*) (second) MMS, (*c*) (third) MHH, (*d*) (fourth) MHS

the subharmonic resonance region shift toward the right with increases in b_1. When the coefficient of the cubic term, b_3, in the heave force component is increased from 0 to 219.6 N/m^3, the response in the secondary resonance region in heave and surge (see [2] for details) is observed to increase for MM and MH and the effects are more pronounced for MH. The observed results are similar to those for varying the coefficient of the cubic term, a_3, in the surge force component.

From Fig. 4, it is found that by varying the coupled restoring force coefficient c_{12}, there is no significant effect on MM. For MH as shown in Figs. 4(*c*) and 4(*d*), the response in the primary resonance region is not affected, but the secondary subharmonic response increases with increase in the coefficients. Similar effects are observed for varying the coupled restoring force coefficient c_{21}.

By varying the linear structural damping coefficient in surge ζ_1 from 0 to 0.1, the subharmonic response decreases with increasing damping and the primary resonance region is not affected, as demonstrated in Fig. 5 and the effects are more noticeable for MH. Similar effects are observed for varying the linear structural damping coefficient in heave ζ_3 (see [2]). Also, a similar trend of decreasing subharmonic response with the increase in coefficients are observed for the nonlinear drag coefficients C'_{d1} and C'_{d3}.

Effects of KC and Re on Hydrodynamic Coefficients. From the optimal range and the most suitable value of Keulegan–Carpenter number KC_F, and Reynolds number Re_F; and inertia and drag coefficients, C_m and C_d, tabulated in Table 1(*a*) in Part 1, it can be observed that the inertia coefficient C_m decreases with increasing KC_F and Re_F, but varying C_d has no effect on the response amplitudes.

MDOF System Superharmonic Behavior

Two tests, MSP1 and MSP2 (where M and SP stand for multi-degree-of-freedom and superharmonic responses, respectively) yielded superharmonic responses [3]. The monochromatic wave period for both tests was doubled to T=8.4 s (f=0.12 Hz). The datasets were labeled and grouped according to the wave amplitude. The wave velocity and acceleration were evaluated using the central difference method [4]. The sampling interval used in the experiment is 0.0625 s, which yields a Nyquist frequency of 8 Hz. The total number of samples for spectral simulations is 8192 (512 s), with subrecord lengths of 1024 for the Fourier transforms (64 s).

Time Series and Spectra. A typical segment of the time series and spectra for the entire record of wave and responses (surge and heave) of test MSP1 are given in Fig. 6 (results for MSP2 are very similar and hence not presented here to avoid repetition). The input wave characteristics such as wave height (H), Keulegen–Carpenter number (KC_F) and Reynolds number (Re_F) and the identified system parameters, a_1, a_2, a_3, b_1, b_3, c_{12}, c_{21}, ζ_1, ζ_3, C_{d1}, and C_{d3} using the R-MI/SO technique are shown in Table 2.

Sensitivity Analysis. A numerical sensitivity analysis was conducted to determine a suitable range of system parameters. Each parameter was varied in specific increments while keeping all the other identified properties constant (see Table 2) and the surge and heave responses were simulated for each parameter set. The results are compared against each other in both the time and frequency domains. The most probable range and value of the system parameters are tabulated in Table 3, and they remain consistent for both MSP1 and MSP2 tests. The observations are summarized through spectral diagrams in the following paragraphs.

The effects of varying the coefficient a_1 of the linear term of the surge restoring force component on heave and surge responses for

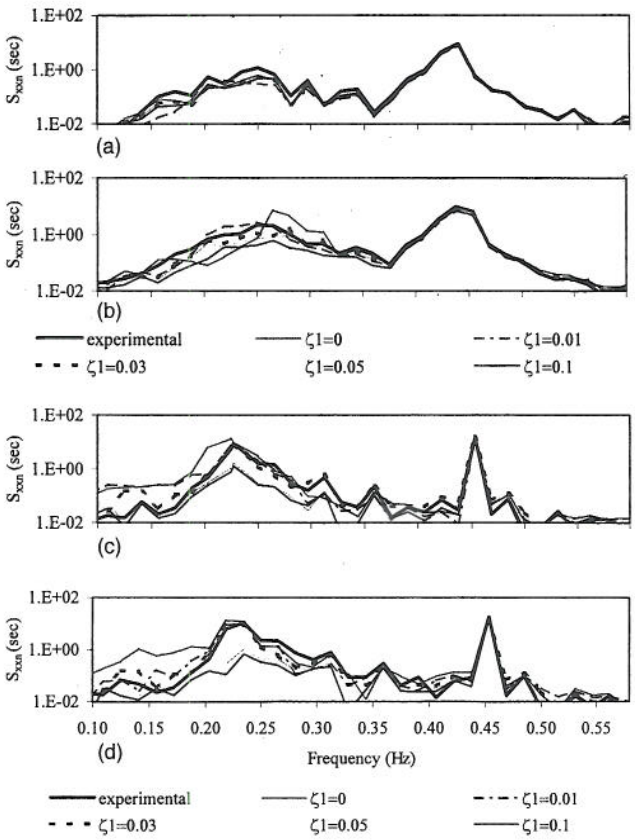

Fig. 5 Effect of ζ_1 on MDOF system behavior: (*a*) (first) MMH, (*b*) (second) MHH, (*c*) (third) MMS, (*d*) (fourth) MHS

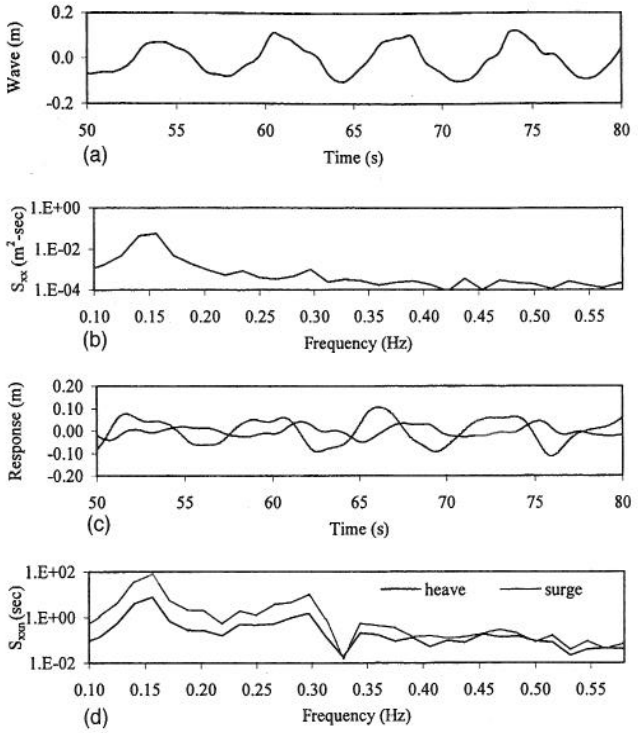

Fig. 6 MDOF experimental data, MSP1: (*a*) (first) wave time series, (*b*) (second) wave spectra, (*c*) (third) response time series, (*d*) (fourth) response spectra

the tests MSP1 and MSP2 are presented in Fig. 7. The spectral density normalized with the variance of measured wave data (S_{xxn}) is plotted against frequency for a_1 from 58.4 to 219.2 N/m or a1n (the ratio of the instantaneous value of a_1 to the best value of a_1, as given in Table 3) from 0.33 to 1.25. The heave response appears unaffected for both tests. For the surge response behavior [Figs. 7(*b*) and 7(*d*)], the primary and secondary response slightly increases with increasing a_1. When the coefficient a_2 of the quadratic term of the surge restoring force component is increased from 0 to 480 N/m^2 (or a2n=0 to 1.25), the response in the secondary resonance (superharmonic) region for surge increases slightly for tests MSP1 and MSP2, as given in Figs. 8(*a*) and 8(*c*). The primary resonance region does not appear to be affected by variations in a_2. The effects of varying the coefficient a_3 of the cubic term of the surge-restoring force component on the identified responses showed (see [2]) that only the response in the secondary resonance region is influenced, which decreases with a_3 (from 0 to 1450 N/m^3 or a3n from 0 to 2.5).

The effects of varying the coefficient b_1 of the linear term of the heave-restoring force component from 1670 to 3390 N/m on the heave and surge responses for test MSP1 and MSP2 are similar to that of varying the coefficient a_1 of the linear term of the surge-restoring force component (see [2]). The surge response does not change significantly for either test. For the heave response, it was observed that the primary and the superharmonic resonance energy increases with increasing b_1.

When the coefficient b_3 of the cubic term of the heave-restoring force component is varied from 0 to 220 N/m^3, the heave and surge responses for either test are not affected (see [2]). Also, by varying the coupled restoring force coefficients, c_{12} and c_{21}, there is no significant influence on the identified responses of tests MSP1 and MSP2 (see [2]). By varying the linear surge structural damping coefficient ζ_1 from 0 to 0.1 (Fig. 9), the amplitude of the superharmonic response decreases with increasing damping values and the primary resonance region does not appear to be affected. A similar observation was made for varying the linear heave structural damping coefficient ζ_3 through that range (see [2]). A similar trend of decreasing superharmonic response with increasing nonlinear damping coefficients can be observed for C'_{d1} and C'_{d3}.

Table 2 Characteristics of the MDOF superharmonic data: wave, (*b*) identified system parameters (SI units)

(*a*)

Data	H (m)	KC_F	Re_F	C_m	C_d
MSP1	0.09	0.81	2.75*e*4	1.4	0.1–0.9 (0.5)
MSP2	0.09	0.90	3.1*e*4	1.4	0.1–0.9 (0.5)

(*b*)

Data	a_1 N/m	a_2 N/m^2	a_3 N/m^3	b_1 N/m	b_3 N/m^3	c_{12} N/m^3	c_{21} N/m^3	$C_{d1,3}$	$\zeta_{1,3}$ %	$f_{n1,3}$ (Hz)
MSP1	173.9	405.7	972.4	180.3	1271.9	1568.1	1806.4	1.2	2.5	0.28
MSP2	173.9	405.7	1020.7	177.1	1178.5	2273.3	2823.9	0.9	3.1	0.28

Table 3 Identified system parameters from the sensitivity analysis of the MDOF superharmonic data (SI units)

Data	MSP1	MSP2
a_1 (N/m)	157.8–193.2 (173.9)	154.6–196.4 (177.1)
a_2 (N/m^2)	264.0–405.7 (334.9)	257.6–412.2 (338.1)
a_3 (N/m^3)	157.8–1725.9 (940.2)	157.8–1725.9 (940.2)
b_1 (N/m)	157.8–190.0 (173.9)	157.8–206.1 (173.9)
b_3 (N/m^3)	157.8–1255.8 (705.2)	157.8–1255.8 (705.2)
c_{12} (N/m^3)	157.8–3606.4 (1883.7)	157.8–3606.4 (1883.7)
c_{21} (N/m^3)	157.8–3606.4 (1883.7)	157.8–3606.4 (1883.7)

Comparing the superharmonic response behavior with that of subharmonic data (explained in the previous section), it can be seen that they exhibit the similar behavior. For data with a smaller amplitude as with the superharmonic responses tests MSP1, MSP2, and the subharmonic responses with medium wave amplitude excitation MM1 and MM2, the effects of sensitivity analysis are not significant compared to the subharmonic responses to low wave amplitudes ML. All of them have similar identified system parameters, however, the range for low wave amplitude data, ML is significantly narrower.

Comparisons of MDOF and SDOF System Behavior

Eight tests were performed on the SDOF configuration using periodic excitation with white noise perturbations [5,6]. Note that as shown in Fig. 10, the rod passing through the centroid of the sphere prevents heave motions and induces slight Coulomb friction in the surge motion. Each of the SDOF tests displayed some evidence of subharmonics in the surge sphere movement (system response). The datasets SL1, SL2, SM1, SM2, SM3, SH1, SH2, and SH3 are grouped according to wave excitation amplitudes, where "*S*" stands for a single-degree-freedom, and "*L*," "*M*," and "*H*" represent low, medium, and high wave amplitudes, respec-

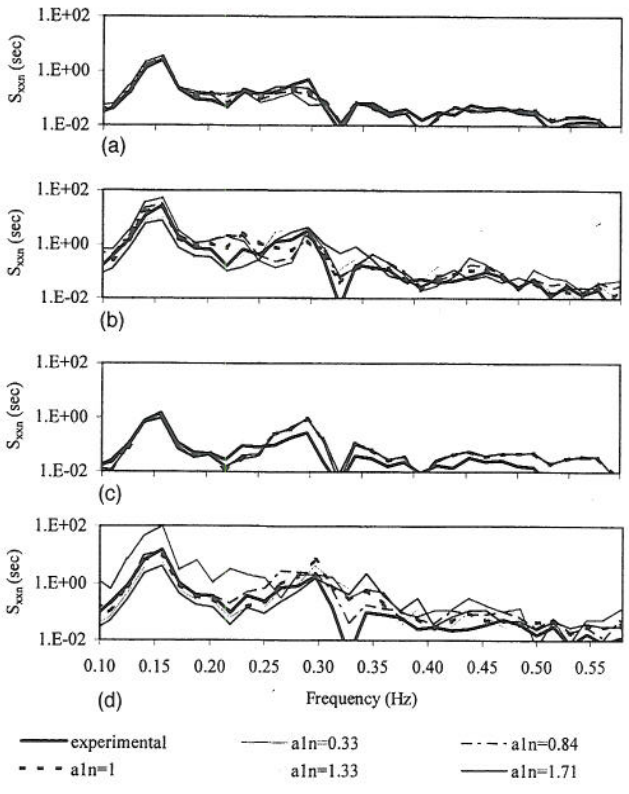

Fig. 7 Effect of a_1 on MDOF system behavior (*a*) (first) MSP1H, (*b*) (second) MSP1S, (*c*) (third) MSP2H, (*d*) (fourth) MSP2S

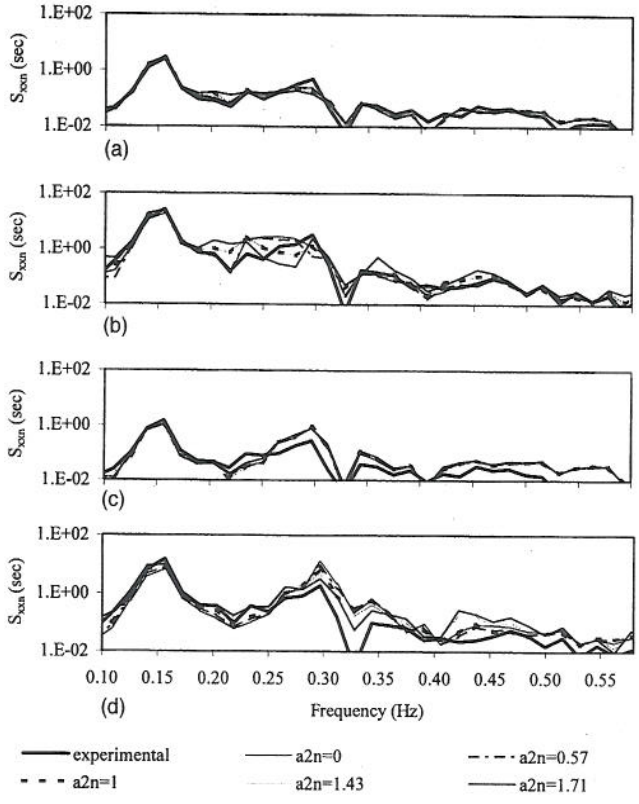

Fig. 8 Effect of a_2 on MDOF system behavior: (*a*) (first) MSP1H, (*b*) (second) MSP1S, (*c*) (third) MSP2H, (*d*) (fourth) MSP2S

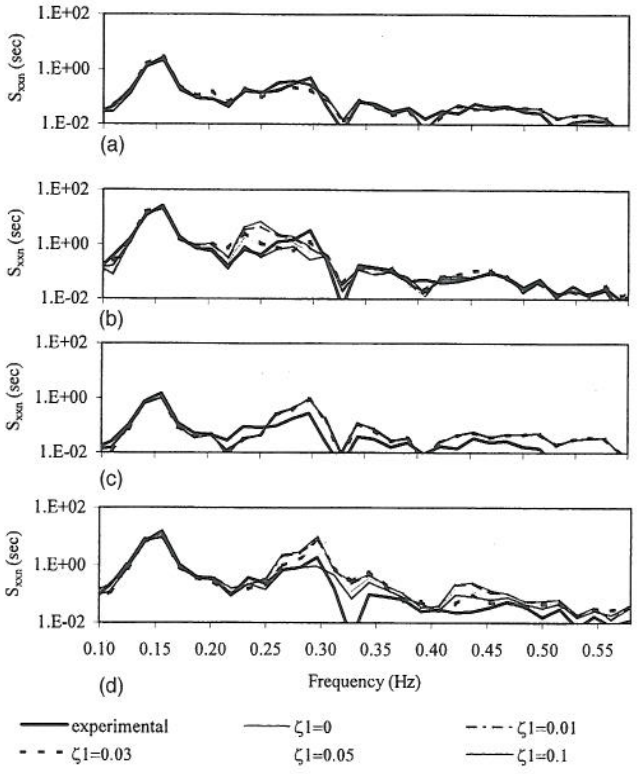

Fig. 9 Effect of ζ_1 on MDOF system behavior: (*a*) (first) MSP1H, (*b*) (second) MSP1S, (*c*) (third) MSP2H, (*d*) (fourth) MSP2S

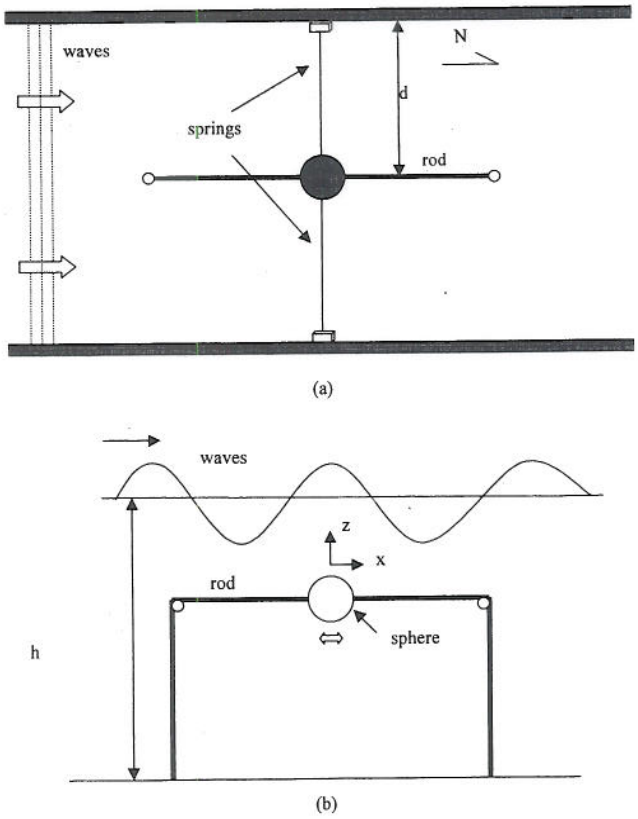

Fig. 10 SDOF experimental setup: (*a*) plan; (*b*) profile view

tively. The wave time series (a typical segment) and spectra, response time series (a typical segment) and spectra for all the datasets grouped are given in Figs. 11–13. The mean spectra for the three groups, SL, SM, and SH are also shown in the figures and are considered to be representative of each group.

All the SDOF system experimental data have a sinusoidal wave period, T=2.0 s and they vary in their wave heights and noise/signal ratio. The input wave characteristics such as wave height (H), C_m, C_d, Keulegan Carpenter number (KC_F) and Reynolds number (Re_F) are shown in Table 4(*a*). The system parameters, i.e., the coefficients of the linear, quadratic and cubic surge restoring force, the linear and nonlinear damping coefficients a_1, a_2, a_3, ζ_1, and C'_{d1}, respectively, identified using the R-MI/SO technique are given in Table 4(*b*).

The SDOF and MDOF subharmonic surge responses are compared below. Specifically, comparisons of the wave excitation and surge response time series, R-MI/SO technique application, identified parameters, results for the sensitivity analysis on surge system parameters, and the effects of varying hydrodynamic coefficients between SDOF and MDOF are presented and discussed.

Time Series, Phase Diagrams and Wave Spectra. From Table 1(*a*) in Part 1 and Table 4(*a*) here, it can be seen that the wave excitation characteristics of MH and SM3 closely match each other; this makes them suitable for comparisons. The time series and spectra of the input and output of these two tests are presented in Fig. 14. It can be observed from the wave spectra that the wave amplitudes match closely, however, there is a slight difference in the wave period. Comparing surge response time series and spectra from Figs. 14(*c*) and 14(*d*), the SM3 response amplitude is smaller in magnitude than MH. This can be attributed to the friction between the rod and the sphere that might have reduced the sphere movement for the SDOF system.

Reverse Multiple-Input/Single-Output (R-MI/SO) Technique Application. In this and a previous study, the R-MI/SO technique has been applied to identify the linear and nonlinear parameters of both the MDOF and SDOF systems. Several alternative MI/SO models have been derived for the SDOF system based on the how each term in the equation is treated either as a mathematical input or output and also depending upon the equation used to represent the hydrodynamic force. The IFF-NSND model has been found to be the most appropriate representation of the SDOF experimental system and has been extended to MDOF

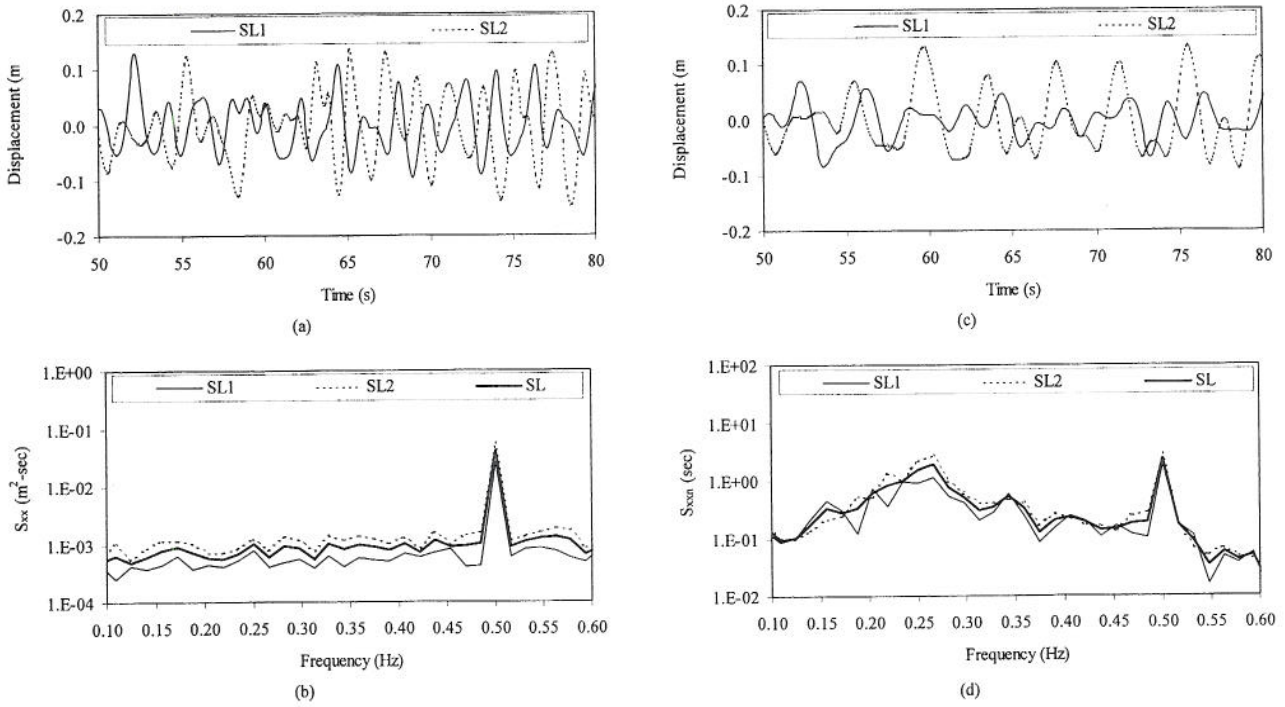

Fig. 11 SDOF experimental low wave amplitude data: (*a*) wave time series, (*b*) wave spectra, (*c*) response time series, (*d*) response spectra

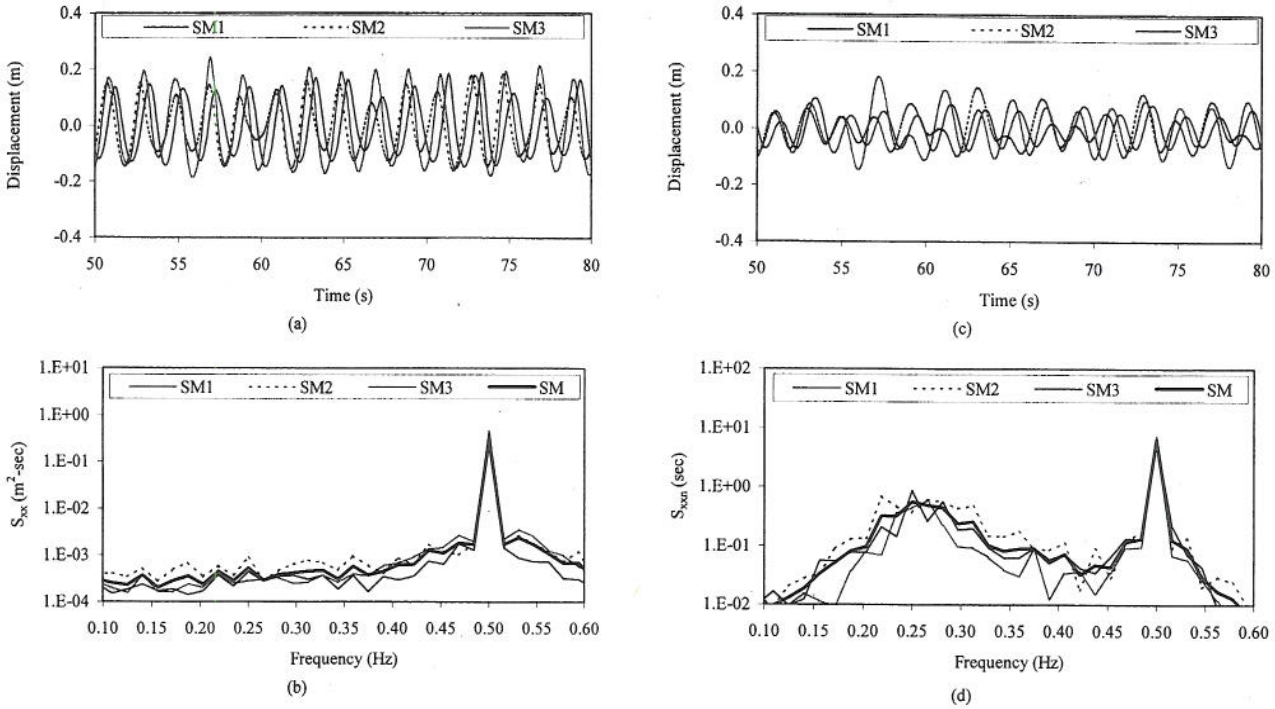

Fig. 12 SDOF experimental medium wave amplitude data: (*a*) wave time series, (*b*) wave spectra, (*c*) response time series, (*d*) response spectra

system in this study. Both models identify system parameters that generate a matching response with that of the experimental data. The formulation of the computational technique is straightforward, simple, and efficient. The standard multiple-input/single-output procedures are incorporated in MATLAB 5.2 [7] and once the program developed for the SDOF model, it can easily be extended to systems with arbitrary degrees of freedom. In this section, the relationship between the surge responses of the MDOF and SDOF systems are investigated.

Identified System Parameters. By restricting the heave response (x_3) to be equal to zero, the governing equations (1)–(9) given for the MDOF surge–heave model is reduced to SDOF surge motion only. This allows for a comparison of the parameters in surge between the SDOF and MDOF systems tabulated in Table 1(*b*) and 4(*b*). In general, it can be observed that the parameters of the MDOF system are larger in magnitude compared to those of the SDOF system. The average natural frequency of the system,

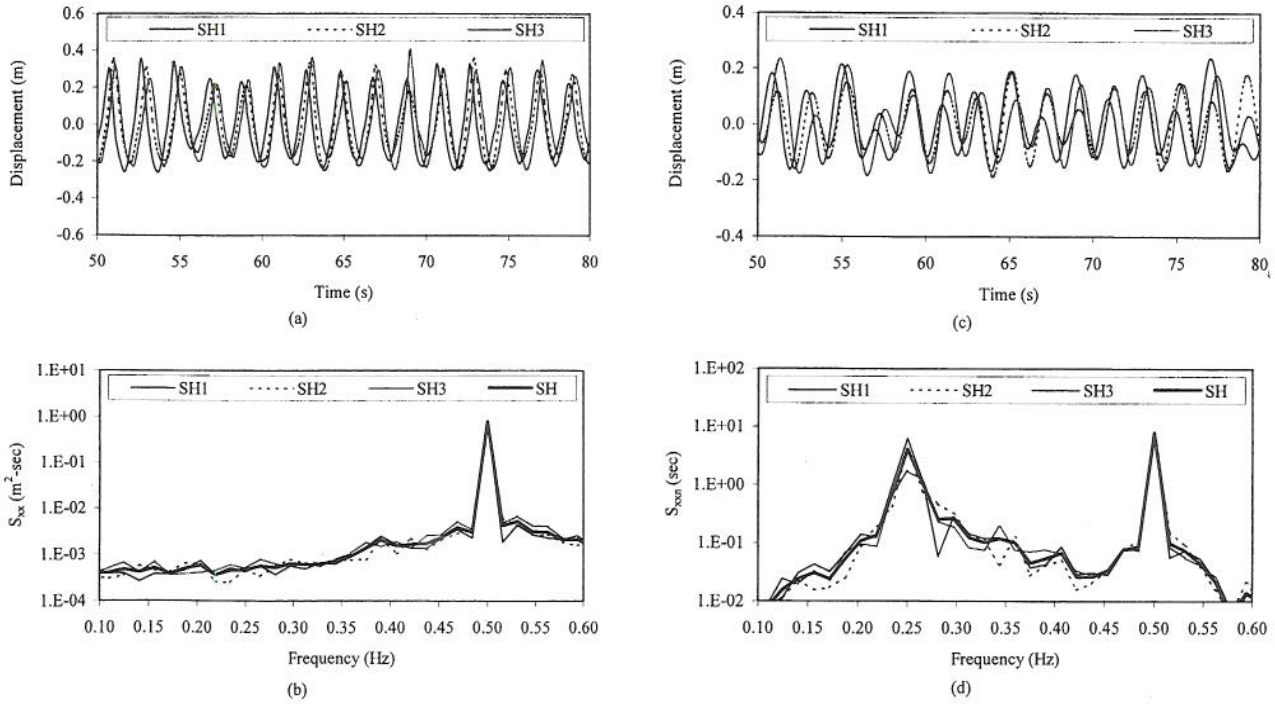

Fig. 13 SDOF experimental high wave amplitude data: (*a*) wave time series, (*b*) wave spectra, (*c*) response time series, (*d*) response spectra

Table 4 Characteristics of the SDOF subharmonic data: wave, (*b*) identified system parameters

(*a*)

Data	H (m)	C_m	C_d	KC_F	Re_F
SL1	0.17	1.4	0.1–0.9 (0.5)	0.56	5.7045
SL2	0.24	1.4	0.1–0.9 (0.5)	0.79	7.80*E*4
SM1	0.35	1.3	0.1–0.9 (0.5)	1.18	1.20*E*5
SM2	0.36	1.3	0.1–0.9 (0.5)	1.18	1.20*E*5
SM3	0.49	1.3	0.1–0.9 (0.5)	1.57	1.60*E*5
SH1	0.66	1.1	0.1–0.9 (0.5)	2.16	2.20*E*5
SH2	0.66	1.1	0.1–0.9 (0.5)	2.18	2.22*E*5
SH3	0.67	1.1	0.1–0.9 (0.5)	2.20	2.30*E*5

(*b*)

Data	a_1 (N/m)	a_2 (N/m^2)	a_3 (N/m^3)	C_{d1}	ζ_1 (%)	f_{n1} (Hz)
SL1	128.8	315.6	721.3	2.5	3.5	0.22
SL2	125.6	280.1	814.7	3.5	3.4	0.23
SM1	128.8	260.8	863.0	3.0	3.0	0.23
SM2	132.0	257.6	769.6	1.5	2.9	0.24
SM3	125.6	206.1	689.1	1.0	2.8	0.23
SH1	128.8	209.3	689.1	0.8	3.0	0.23
SH2	128.8	209.3	689.1	0.2	3.2	0.23
SH3	125.6	190.0	627.9	0.3	3.1	0.22

f_{n1} identified using the MDOF data is 0.28 Hz and that of the SDOF system is 0.23 Hz. The nonlinear structural damping coefficient, Cd_1', varies among the three groups of SDOF data, SL, SM, and SH, this could be due to the presence of a rod in the SDOF system, which affects the "Coulomb" damping not included in the MDOF system modeling [5,6].

Sensitivity Analysis. Based on sensitivity analyses for the MDOF and SDOF systems [6], it can be observed that varying the surge system parameters (a_1, a_2, a_3, ζ_1, and C_{d1}') have similar effects on the SDOF and MDOF systems. Similar to the MDOF tests where there are three categories of data (depending on low, medium or high wave excitation amplitude) that exhibit similar behaviors within each category, the SDOF tests are also grouped into three categories. However, there are more experimental test for the SDOF system available to confirm the surge response behavior.

Effects of KC and Re on Hydrodynamic Coefficients. The application of the R-MI/SO technique on SDOF and MDOF, NSND models require a priori values of the drag and inertia coefficients C_d and C_m for the evaluation of hydrodynamic force on the sphere. The dependence of the inertia coefficient, C_m, on Reynolds number (Re_F) and Keulegan-Carpenter number (KC_F) for

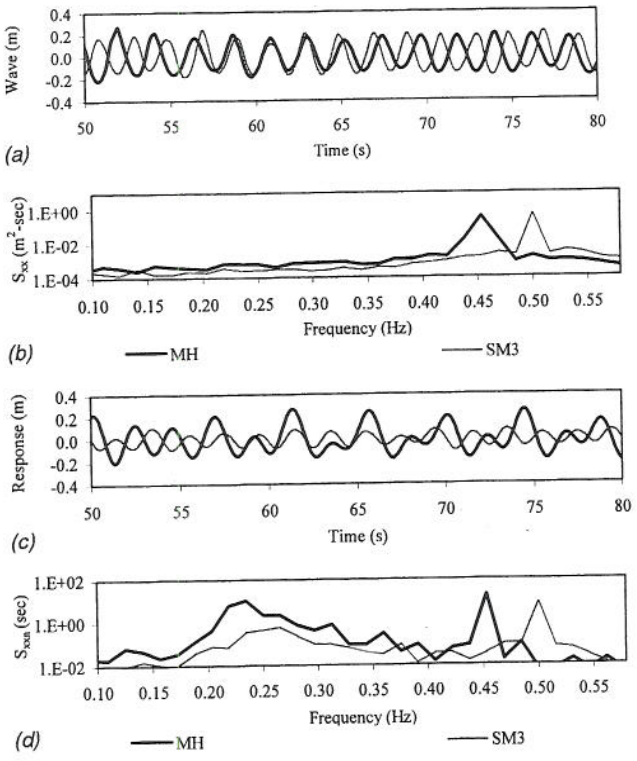

Fig. 14 Comparison of MDOF and SDOF data: (*a*) (first) wave time series, (*b*) (second) wave spectra, (*c*) (third) surge time series, (*d*) (fourth) surge spectra

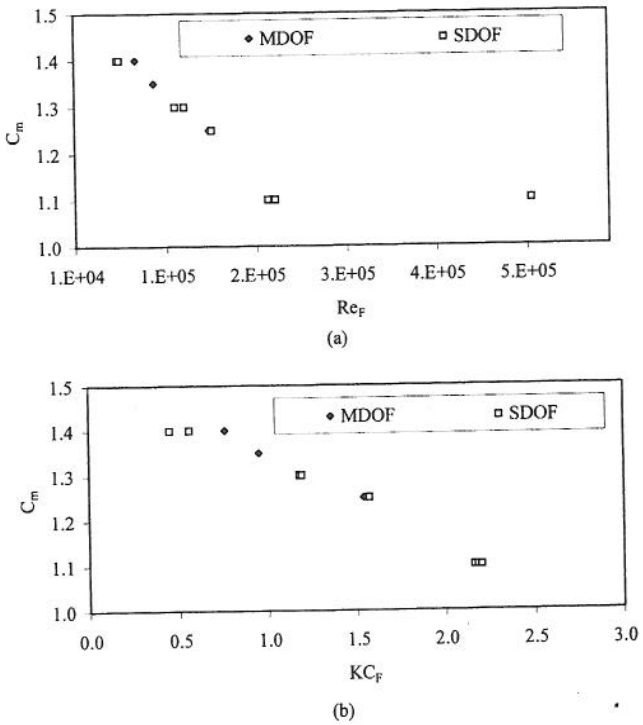

Fig. 15 Effect of C_m and C_d on Reynolds and Keulegan Carpenter numbers: (*a*) Re_F, (*b*) KC_F

the MDOF and SDOF systems are given in Fig. 15. Both sets of coefficients display a similar trend with C_m, decreasing with the increase in Re_F and KC_F, and vary between 1.4–1.1 for $1.34 \times 10^5 \leq Re_F \leq 5.21 \times 10^5$ and $1.19 \leq KC_F \leq 4$. Wave basin tests on a vertical cylinder [8] show that C_m decreases from 2.4 to 2 with the increase of KC_F from 1 to 6 and also decreases with an increase in Re_F. Tests with spheres show the same coefficient pattern with the lower range of magnitude. From the numerical sensitivity studies, it was found that the predicted response was insensitive to variations in C_d within the range of 0.1 to 1.1. Based on the water depth to wavelength (h/L) and diameter to wave height (D/H) ratios [9], the inertia effects dominate the total forces for both MDOF and SDOF systems. Hence, it is not possible to accurately determine the exact value of C_d.

Discussion

No superharmonic response motions were observed in the SDOF system case. However, the MDOF experimental system exhibited both subharmonic and superharmonic response behavior. This shows that the MDOF system model is essential for an analysis of the response of the moored submerged structure.

For the SDOF data, the most probable range and value for the nonlinear structural damping coefficient identified using the R-MI/SO procedure varied among the tests. This scatter is likely caused by the inability of the model to accurately represent the actual nonlinear damping mechanism of the SDOF configuration, (e.g., the Coulomb frictional component is not included in the mathematical model). The nonlinear effects appear to become more prominent at the lower wave amplitudes, resulting in high values, with the errors lumped in the coefficient, C'_{d1} [5,6]. This pattern was not observed in the MDOF system.

Concluding Remarks

Experimental tests were conducted on a multipoint moored submerged sphere. The resulting subharmonic and superharmonic responses are examined in detail in this study. Using parameters identified by the R-MI/SO technique, a sensitivity analysis was performed on the MDOF system. The subharmonic surge response of MDOF system was then compared to that of the SDOF system.

The sensitivity analysis performed on the MDOF system responses revealed that the effects of varying the system coefficients become more significant with an increasing wave excitation amplitude. The set of most probable values of the system parameters is practically identical for the tests subject to medium- and high-amplitude excitation, but the high-amplitude response has a restricted range. Increasing surge and heave stiffness (restoring force) parameters a_1, a_2, a_3, b_1, and b_3 has the effect of varying the subharmonic energy and shifting the surge and heave response (peak frequency) region. The primary response was not significantly affected. The subharmonic responses increase with the increase in coupled parameters, c_{12} and c_{21}, and decrease with the linear (ζ_1 and ζ_3) and nonlinear (C'_{d1} and C'_{d3}) damping parameters.

Comparing the sensitivity analysis results for the tests that exhibited superharmonic responses versus those with subharmonic responses, it was observed that both exhibit similar response behavior versus parameter variations. In general, the effects were more significant as the wave amplitude increased.

A comparison between the restricted MDOF and SDOF surge response time series and spectra showed that the response amplitude is comparatively smaller for the SDOF system for comparable wave excitation amplitudes. This is attributed to the Coloumb friction from the rod passing through the center of the sphere in the SDOF case.

For the experimental data considered for both configurations, C_m varies between 1.1–1.3 for $5.3 \times 10^5 \leq Re_F \leq 7 \times 10^5$ and $4.7 \leq KC_F \leq 6.2$ and 1.3–1.5 for $1.3 \times 10^5 \leq Re_F \leq 3.7 \times 10^5$ and $1.2 \leq KC_F \leq 3.3$. In general, C_m increases with the decrease in Reynolds number and Keulegen–Carpenter number. These values are consistent with that of cylinders observed in the literature. Since the experimental wave characteristics fall within the inertia regime, it was not possible to accurately evaluate the drag coefficients. Indeed, the response is observed to be insensitive to variations in C_d.

Acknowledgment

Financial support from the U.S. Office of Naval Research, (Grants No. N00014-92-J-1221 and No. N00014-04-10008), is gratefully acknowledged.

References

[1] Raman, S., Yim, S. C. S., and Palo, P. A., 2005, "Sub- and Super-Harmonic Responses of a MDOF Moored Structure, Part 1—Nonlinear System Identification," ASME J. Offshore Mech. Arct. Eng., **127**, 283–290.

[2] Narayanan, S., 1999, "Experimental Analysis of a Nonlinear Moored Structure," Ph.D. dissertation, Oregon State University.

[3] Yim, S. C. S., Myrum, M. A., Gottileb, O., Lin, H., and Shih, I-M., 1993, "Summary and Preliminary Analysis of Nonlinear Oscillations in a Submerged Mooring System Experiment," Ocean Engineering Report No. OE-93-03, Office of Naval Research.

[4] Gerald, G. F., and Wheatley, P. O., 1989, *Applied Numerical Analysis*, Addison-Wesley, New York.

[5] Narayanan, S., and Yim, S. C. S.,2004, "Modeling and Identification of a Nonlinear SDOF Moored Structure, Part I, Hydrodynamic Models and Algorithm," ASME J. Offshore Mech. Arct. Eng., **126**, pp. 175–182.

[6] Yim, S. C. S., and Narayanan, S., 2004, "Modeling and Identification of a Nonlinear SDOF Moored Structure, Part II, Comparisons and Sensitivity Study," ASME J. Offshore Mech. Arct. Eng., **126**, pp. 183–190.

[7] MATLAB 6.5.1, The Math Works, Inc., 1994–2004.

[8] Chakrabarti, S. K., 1987, *Hydrodynamics of Offshore Structures*, Computational Mechanics Publications, London.

[9] Harleman, D. R. F., and Shapiro, W. C., 1958, "Investigations on the Dynamics of Moored Structures in Waves," M.I.T. Hydrodynamics Lab. Tech. Report No. 28.